Petroleum Science 19 (2022) 2165–2174

Contents lists available at ScienceDirect

Petroleum Science

journal homepage: www.keaipublishing.com/en/journals/petroleum-science

Original Paper

Self-aggregating behavior of poly(4-vinyl pyridine) and the potential in mitigating sand production based on π-π stacking interaction

Jian-Da Li [a], Gui-Cai Zhang [a, *], Ji-Jiang Ge [a], Wen-Li Qiao [a], Hong Li [b], Ping Jiang [a], Hai-Hua Pei [a]

[a] School of Petroleum Engineering, China University of Petroleum (East China), Qingdao, 266580, Shandong, PR China
[b] College of Pharmacy, Shandong University of Traditional Chinese Medicine, Jinan, 250000, Shandong, PR China

ARTICLE INFO

Article history:
Received 23 December 2021
Received in revised form
1 June 2022
Accepted 1 June 2022
Available online 3 June 2022

Edited by Yan-Hua Sun

Keywords:
Self-aggregating
Poly(4-vinyl pyridine)
π-π stacking
Sand migration control

ABSTRACT

Unconsolidated sandstone reservoirs are most susceptible to sand production that leads to a dramatic oil production decline. In this study, the poly(4-vinyl pyridine) (P_4VP) incorporated with self-aggregating behavior was proposed for sand migration control. The P_4VP could aggregate sand grains spontaneously through π-π stacking interactions to withstand the drag forces sufficiently. The influential factors on the self-aggregating behavior of the P_4VP were evaluated by adhesion force test. The adsorption as well as desorption behavior of P_4VP on sand grains was characterized by scanning electron microscopy and adhesion force test at different pH conditions. The result indicated that the pH altered the forms of surface silanol groups on sand grains, which in turn affected the adsorption process of P_4VP. The spontaneous dimerization of P_4VP molecules resulting from the π-π stacking interaction was demonstrated by reduced density gradient analysis, which contributed to the self-aggregating behavior and the thermally reversible characteristic of the P_4VP. Dynamic sand stabilization test revealed that the P_4VP showed wide pH and temperature ranges of application. The production of sands can be mitigated effectively at 20–130 °C within the pH range of 4–8.

1. Introduction

Most world's hydrocarbons are located in unconsolidated reservoirs, in which rocks are usually relatively young in geologic age, and are unconsolidated because natural processes have not cemented the rock grains together by mineral deposition (Abanum and Appah, 2013; Kalgaonkar et al., 2017; Styward et al., 2018). Unconsolidated sandstone reservoirs are most susceptible to sand production, especially in cases that involve sufficient changes of *in-situ* stresses, high oil production rates, collapse of hole cavities, and presence of water in the formation (Ranjith et al., 2013). Excessive sand production can erode subsurface equipment, wear surface production facilities, increase production cost, cause sudden choking of wells and create down-hole cavities leading to the closure of an entire field (Chaloupka et al., 2010; Fuller et al., 2011; Zaitoun et al., 2009).

Generally speaking, sand control can be achieved by three mechanisms: reducing drag force, bridging sand mechanically, and increasing formation strength (Marfo et al., 2015). Various techniques and methods have been successfully employed to produce oil and gas from poorly consolidated reservoirs based on this guiding principle. Mechanical techniques including stand-alone screens, slotted-liners, gravel packs, and frac-pack treatments are trustworthy in providing sand control (Ma et al., 2020; Ott and Woods, 2003). However, these techniques are usually costly, especially for short treated intervals or for wells with a short expected economic lifetime (Kuma and Affeld, 2018). The chemical sand consolidation method is regarded as an approach to tackle sand production problem from the root (Talaghat et al., 2009). The main purpose of sand consolidation is to strengthen the formation in the immediate area of the wellbore with a chemical that will bind together the partially consolidated or unconsolidated grains at their point of contact (Marfo et al., 2015). The traditional sand consolidating agents like resins attempt to restore the strength of the rock matrix to a large degree by chemical consolidation but have been shown to be faced with some problems such as relative

* Corresponding author.
E-mail address: zhangguicaiupc@126.com (G.-C. Zhang).

https://doi.org/10.1016/j.petsci.2022.06.001

permeability reduction, multiple and multistage injections (Dupuis et al., 2016; Mishra and Ojha, 2016; Tabbakhzadeh et al., 2020). In recent years, the advanced practice in sand control aims to improve the residual strength of the formation and hence the maximum sand free rate (MSFR) instead of emphasizing on consolidation strength (Li et al., 2017). Based on this concept, a variety of additives have been developed, including cationic polymers, nanoparticles, organosilanes, polyacrylamide hydrogels and zeta potential altering agents (Alakbari et al., 2020; Hafez et al., 2011; Liu et al., 2016; Mahardhini et al., 2015; Marandia et al., 2018; Ogolo et al., 2013). Although these methods have proved feasible and able to minimize the coproduction of formation sands in different degree, it is still necessary to find better methods and systems.

Poly(4-vinyl pyridine) (P_4VP) is a neutral polymer and has very interesting properties coming from the pyridine rings. The unique properties of the pyridine rings together with the further modifiability of the nitrogen atoms by the addition of various chemistries to the repeating units are crucial for advanced material design (Arslan and Saraydin, 2017). Although the P_4VP and its derivatives have been successfully used as ion-exchange membranes, bactericide, adsorbents, ion conductors and polymer-supported catalyst (Albadi et al., 2012; Chetia et al., 2004; İşoğlu1 et al., 2018; Kawabata and Ohira, 1979; Stachera and Childs, 2001), they still show great potential in formation sand consolidation. In terms of being a sand consolidating agent candidate, the P_4VP is insoluble in water or alkane. Besides, the sand grains with the treatment of P_4VP will bind together through the π-π stacking interactions between P_4VP molecules to withstand the drag forces sufficiently, resulting in less co-production of formation sands. In general, π-π stacking interaction is a reversible, spontaneously forming noncovalent interaction, existing between the overlapping portions of the aromatic rings or derived heterocyclic rings due to a set of out-of-plane *p* electrons (Son et al., 2018). The π-π stacking interaction is essentially a weak van der Waals force, hence, the P_4VP is aimed to form a relative weak physical consolidation rather than solid consolidation as traditional resins. In addition, it is noteworthy that the reversible π-π stacking interactions in P_4VP molecules endow the sand grains with spontaneous, and reversible agglomerate property. Once the agglomerated sand grains are scattered due to the formation stress changes resulting from reservoir depletion or other factors, they can adapt to the resultant changing reservoir conditions and re-agglomerate, which will extend the life expectancy of the sand migration control.

In this study, the P_4VP incorporates with self-aggregating behavior is proposed for mitigating sand production based on reversible π-π stacking interaction. Furthermore, the series of properties of the P_4VP including the aggregation strength, adsorption/desorption behavior, dynamic sand stabilization performance, and functional mechanisms are analyzed.

2. Experimental

2.1. Materials

The P_4VP (95% purity, $\overline{M}_w = 200 - 300$) was obtained from Tongkun Petroleum Technology Co., LTD. Dodecylphenol ethoxylates (DPEO, 98% purity) was supplied by Jiangsu Hai'an Petrochemical Plant. Ethanol (99.5% purity), ethylene glycol butyl ether (EB, 98.5%), potassium chloride (KCl, 99.8% purity), sodium hydrogen carbonate (Na_2CO_3, 99.5% purity), hydrochloric acid (HCl, 36.0%–38.0% purity) and mineral oil were purchased from Sinopharm Chemical Reagent Co., Ltd. The viscosity–temperature curves of the mineral oil are shown in Fig. 1. Quartz sands (0.104–0.117 mm) and quartz microspheres (0.35 mm) obtained from Shili Abrasive Industry were cleaned with 5 wt% HCl solution, 1 wt% H_2O_2 solution and distilled water in turn.

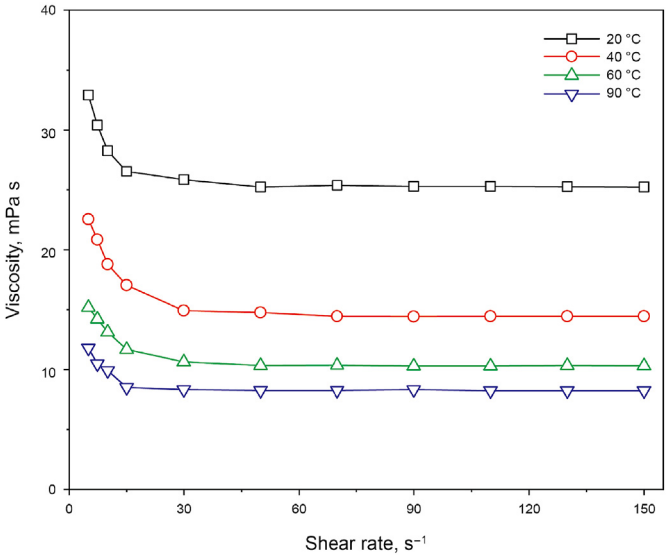

Fig. 1. The viscosity–temperature curves of the mineral oil.

2.2. Methods

2.2.1. Preparation of P_4VP dispersion

The P_4VP dispersion is prepared at room temperature according to the following steps. Firstly, the P_4VP-ethanol solution with a P_4VP concentration of 20 wt% is prepared by dissolving P_4VP powder in ethanol. Secondly, the P_4VP-ethol solution and the dispersing agents including DPEO and EB are mixed in a blender at a speed of 500 r/min with a mass ratio of 2:1:1. Then distilled water is slowly added to the blender and keeps stirring for another 2 min. The mass fraction of the P_4VP in the dispersion is 1 wt%. The static stability of the P_4VP dispersion is evaluated by dynamic light scattering. As revealed in Fig. 2, the mean grain size of the fresh P_4VP dispersion increases from 22.3 to 124.6 nm after being settled for 24 h, showing a favorable static stability at room temperature.

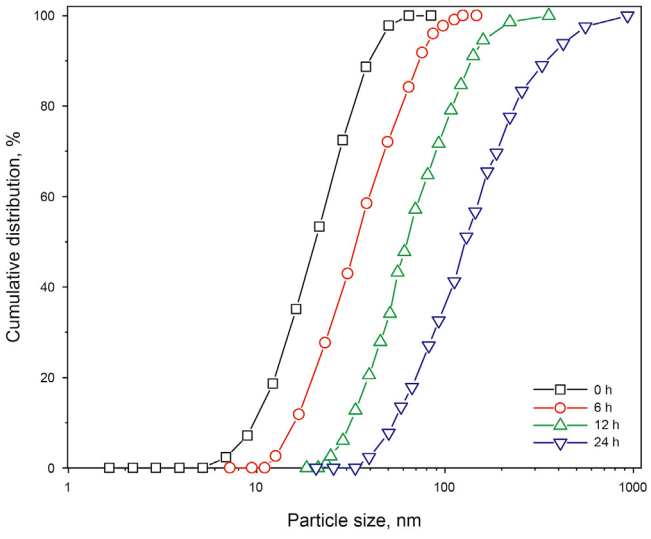

Fig. 2. Particle size distribution changes with settling time.

2.2.2. Characterization

The zeta potential of ground sand grains at different pH conditions is determined by NanoBrook 90Plus PALS. The surface morphology and the elemental composition of the P_4VP-treated sand grains are characterized by scanning electron microscopy (SEM, Hitachi SU3500) and energy dispersive spectroscopy (EDS).

An adhesion force testing apparatus (Fig. 3) is set up to quantitatively characterize the aggregation strength between the P_4VP-treated sand grains (Song et al., 2010). Considering that the results of the adhesion force test are quite influenced by the regularity of the particles, hence, regular-shaped quartz microspheres are optimized to simulate the sand grains to reduce the experimental error. Adhesion force tests are conducted using the following procedure. (1) Two quartz microspheres are fixed separately at the bottom of the pressure transducer and the tip of the probe. (2) The pressure transducer and the probe are immersed in the P_4VP dispersion and soaked for 6 h. Then replace the P_4VP dispersion with distilled water or aqueous solution of different pH values. (3) Adjust the pressure transducer and the probe to move toward each other. The reading of the pressure transducer is set to zero when slight contact is established between the quartz microspheres. (4) After resting for 30 min, the quartz microspheres are separated at a fairly low velocity (0.1 mm/s). (5) Record peak force during the separation process as the adhesion force between the P_4VP-treated quartz microspheres. (6) Repeat the steps (3)–(5) and record the adhesion force changes during continuous contact-separation cycles.

2.2.3. Computational details

Considering that the intricate noncovalent interactions of complex molecules cannot be easily identified by conventional experimental methods, first-principles calculations are carried out so as to clarify the noncovalent interactions between the P_4VP molecules (Huang et al., 2021). In view of that the P_4VP is composed of repetitive 4-vinyl pyridine units, the molecular chain of P_4VP is simplified as a short chain with six 4-vinylpyddine units to facilitate the computation. The geometry optimization and the binding energy calculation of the P_4VP dimer are implemented by Gaussian 09 software package at B3LYP/6-311 + G (d, p) level (Frisch et al., 2009; Li et al., 2020). Reduced density gradient (RDG) analysis is performed with the Multiwfn 3.7 program (Lu and Chen, 2012) and plotted using VMD software (Humphrey et al., 1996).

2.2.4. Dynamic sand stabilization performance evaluation

The P_4VP dispersion aims to be applied in the production well treatment to reduce the risk of well failure caused by continuous sand production. Hence, the dynamic sand stabilization performance should be taken into consideration. The test method employed in this study involves flowing brine through a consolidated sand pack and monitoring the sand production in the effluent. Due to the sand consolidation agents inevitably sacrifice permeability to increase consolidation strength, the damage of P_4VP to formation permeability is determined. Sand packs used for displacement tests are 2.5 cm in diameter and 20.0 cm in length. Quartz sand grains of 0.104–0.117 mm are packed to acquire similar porosity (33.0 ± 2.0%) and permeability (2.3 ± 0.2 μm^2) for all the tests. Sand packs are horizontally placed during the displacement process with flexible screens in each end. (Fig. 4). The MSFR and permeability retention rate of the sand packs are evaluated as follows:

(1) To create the condition of residual oil, the sand packs are saturated with mineral oil after being saturated with 2 wt% KCl brine, and then water flooding is conducted until no mineral oil flows out.
(2) Displace the sand packs with 2 wt% KCl brine. Record the balanced inlet pressure at different flow rates and calculate the initial permeability of the sand pack k_1.
(3) One pore volume (PV) of P_4VP dispersion is injected into the sand pack at a flow rate of 1 mL/min in the reverse direction. Then both inlet and outlet were closed for 6 h to simulate the well shut-in process.
(4) Displace the sand packs with 2 wt% KCl brine. Record the balanced inlet pressure at different flow rates and calculate the permeability after treatment k_2. The permeability retention rate is determined as the ratio of k_2 to k_1.
(5) Keep displacing the sand packs with 2 wt% KCl brine. The initial flow rate is set as 5 mL/min and increases in 5 mL/min steps up to 200 mL/min. The flow rate is recorded as the MSFR when the sand grains are found in the effluent. The tests are conducted at 20–150 °C.

3. Results and discussion

3.1. Evaluation of self-aggregating property of P_4VP

3.1.1. Self-aggregating behavior

Self-aggregating behavior of P_4VP refers to the formation sands that will aggregate spontaneously when treated with P_4VP. In addition, once the aggregated sand grains are scattered due to the formation stress changes resulting from reservoir depletion or other factors, they can adapt to the changing reservoir conditions and re-aggregate.

Self-aggregating behavior of P_4VP as well as the aggregation strength of the P_4VP-treated sand grains is characterized by adhesion force test at 20 °C. As mentioned above, regular-shaped quartz

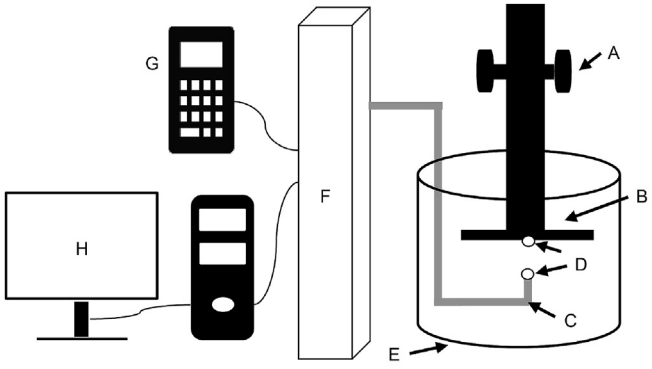

A–Mechanical knob, B–Pressure transducer, C–Probe, D–Quartz microspheres, E–Water bath, F–Motorized *z*-axis stage, G–Control panel, H–Computer

Fig. 3. Schematic of adhesion force testing apparatus.

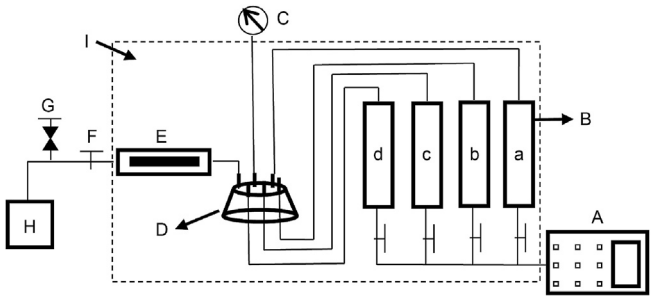

A–Constant flux pump, B–Intermediate container, C–Piezometer, D–Six-way valve, E–Sand pack, F–Check valve, G–Back pressure regulator, H–Sample collection beaker, I–Oven
a–KCl brine, b–Mineral oil, c–HCl solution, d–Na_2CO_3 solution

Fig. 4. Flow chart of the sand pack displacement test.

microspheres are optimized to simulate the sand grains to reduce experimental errors. The adhesion force changes during continuous contact-separation cycles in distilled water are revealed by Fig. 5. As can be seen, there is a slight decline in the adhesion force in the first few cycles, which might result from the uneven distribution of the P_4VP adsorption layer during the separation process, and then it hardly changes during the subsequent contact-separation processes. The adhesion force is 86.5% of the original force after being contacted and separated 20 times and then remains almost constant, indicating the spontaneous, and reversible self-aggregating behavior of the P_4VP.

3.1.2. *Influential factors on the aggregation strength*

In view of the potential challenges posed by formation conditions, the influence of pH and temperature on the aggregation strength of the P_4VP-treated sand grains should be taken into consideration. To evaluate the influence of pH on aggregation strength, the adhesion force tests are conducted in aqueous solution with different pH values at 20 °C. Fig. 6 represents the adhesion force variation between the P_4VP-treated quartz microspheres at different pH conditions. The adhesion force is at its maximum when pH = 5 and then shows a decline as the pH changes. The adhesion force only drops by about 13% when the pH value fluctuates within the range of 4–8, indicating that the weak acidic or alkaline conditions exert a limited influence on the aggregation strength of the treated quartz microspheres. By contrast, the strong acidity or the strong alkalinity impairs the aggregation strength severely. The adhesion force reduces rapidly from about 200 mN to 0 when the pH value decreases from 4 to 1. A similar phenomenon occurs when the pH value increases from 8 to 14. It can be concluded that the self-aggregating behavior of the P_4VP almost disappears in harsh pH conditions given that the adhesion force between the treated quartz microspheres almost reduces to zero.

The aggregation strength between the P_4VP-treated quartz microspheres at different temperatures is explored afterwards. The tests are conducted in a distilled water bath during a heating-cooling cycle in the range of 20–90 °C. As depicted in Fig. 7, the adhesion fore between the treated quartz microspheres is trending downward with the increasing temperature. The adhesion force reduces to 104 mN at 90 °C, indicating the aggregation strength

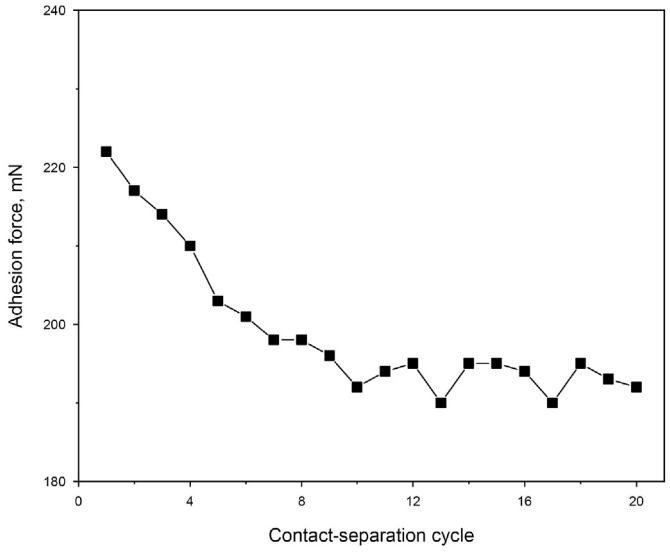

Fig. 5. Adhesion force change during contact-separation cycles.

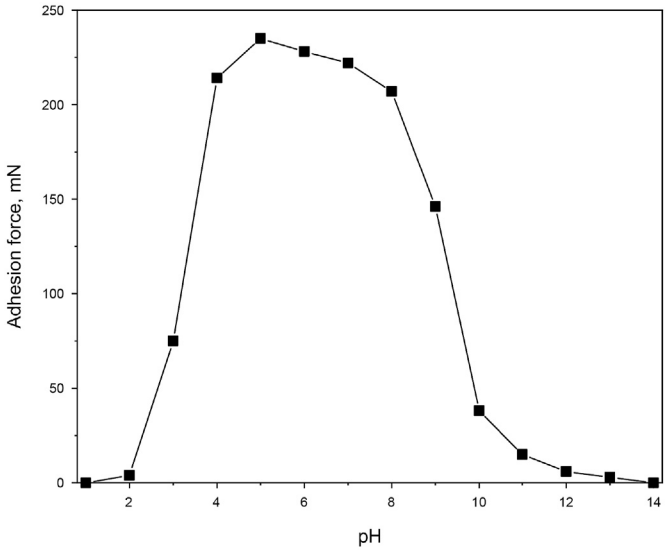

Fig. 6. Adhesion force variation with the pH value.

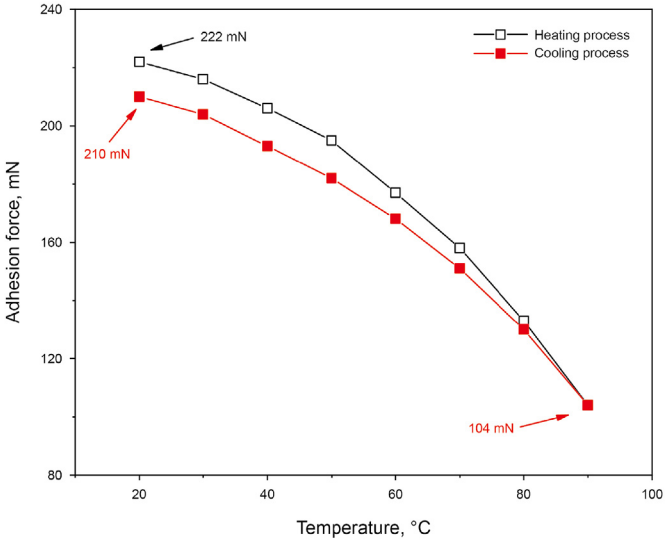

Fig. 7. Adhesion force changes during heating-cooing cycle.

between the treated quartz microspheres is drastically weakened by high temperature. The strength recovery occurs during the cooling process. The regained adhesion force is up to 210 mN when the temperature cools to 20 °C. This value is very close to the initial adhesion force at 20 °C (222 mN), signifying the aggregation strength between the treated quartz microspheres almost completely recovered during the cooling process. Although the adhesion force tests at higher temperature cannot be proceeded subject to the instrument, the thermally reversible characteristic of the P_4VP is predictable.

The self-aggregating process of P_4VP should consist of two steps according to the adhesion force testing procedure. Firstly, the P_4VP will adsorb on the surface of the sand grains and form an adsorption layer. Then the sand grains will aggregate through intermolecular interaction between the adsorbed P_4VP layers. The adhesion force reduction in harsh pH and temperature conditions might be resulted from the collapse of either step.

3.2. Analysis of self-aggregating process of P_4VP

3.2.1. Adsorption/desorption behavior of P_4VP

In the P_4VP-sand grain system, the nitrogen atoms in the pyridine rings might form intermolecular hydrogen bonds with the surface silanol group (Si—OH) of the sand grains, which contributes to the adsorption of P_4VP. However, in terms of the aluminosilicates, the different forms of surface silanol groups including Si—OH, -Si—OH_2^+ and Si—O^- are dominated by the zero charge points (ZPCs) (Zhao, 2001). Here, zeta potentials of the ground sand grains at different pH conditions are tested to determine the ZPC. According to Fig. 8, the ZPC of the sand grains is located at pH = 4–5. The surface of the sand grains is electrically neutral, and the P_4VP tends to adsorb on those by forming intermolecular hydrogen bonds with the surface Si—OH (Malynych et al., 2002; Fujii et al., 2010). When the pH is lower than 4, the surface of sand grains is positive charged since the surface Si—OH combines with H^+ and forms Si—OH_2^+. What is worse, once the P_4VP-treated sand grains are exposed to high-acidity aqueous solutions, the water solubility of P_4VP will be greatly enhanced due to the protonation of pyridine rings, leading to the desorption of the P_4VP (Tantavichet et al., 2001; Wang and Zhao, 2007). When the pH is higher than 5, the surface of sand grains turns gradually negative charged because the surface Si—OH combines with OH^- and forms Si—O^-. With the pH rising constantly, the high-alkalinity condition leads to the complete rupture of the intermolecular hydrogen-bonding interactions between the surface Si—OH and P_4VP molecules, resulting in the desorption of the P_4VP (Malynych et al., 2002).

To verify the adsorption/desorption behavior of P_4VP at different pH conditions, the surface morphology as well as the elemental composition of the sand grains before and after the treatment with P_4VP are characterized by SEM and EDS (Fig. 9). By comparing Fig. 9a and b, an obvious thin film is attached on the surface of P_4VP-treated sand grains when pH = 5. Meanwhile, a new C-peak (0.27 eV) and a new N-peak (0.39 eV) are found in the EDS spectra of the P_4VP-treated sand grains (Fig. 10a, Fig. 10b), indicating that the attached thin film should be the adsorbed P_4VP layer. It makes sense that the adhesion force between the P_4VP-treated quartz microspheres collapses under the high-acidity conditions in view of the desorption of the P_4VP at pH = 2 (Fig. 9c). This argument is supported by the EDS spectra (Fig. 10a and c). The surface elemental composition of the P_4VP-treated sand grains at pH = 2 is almost the same as the untreated sand grains. C-peak and N-peak attributed to P_4VP are not found in the EDS spectra at pH = 2 given that the protonated P_4VP is detached from the surface of the sand grains and dissolves in strong acidic aqueous solution. By comparing Fig. 9b and d, it can be clearly observed that the smooth, continuous adsorption layer turns into rough, irregular deposit sediments when the pH value increases from 5 to 12. The C-peak and N-peak found in the EDS spectra verify that the clusters should be the accumulated P_4VP (Fig. 10d). The surface Si—OH of sand grains turns into Si—O^- in high-alkalinity condition and the intermolecular hydrogen bonds with pyridine ring are broken, leading to the desorption of the P_4VP. However, due to the poor water solubility, the desorbed P_4VP will cement on the sand grains and form irregular deposit sediments.

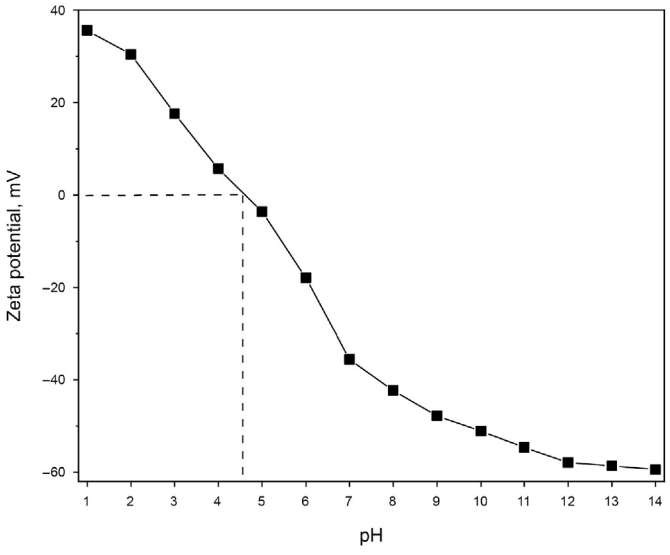

Fig. 8. Zeta potential of sand grains at different pH conditions.

In summary, the presence of strong acidity or alkalinity disrupts the hydrogen-bonding interactions between the P_4VP and the surface Si—OH of sand grains, leading to the desorption of the P_4VP, and thereby threatens the self-aggregating behavior of P_4VP as well as the aggregation strength of the treated sand grains. The supposed adsorption and desorption process are described in Fig. 11.

3.2.2. Spontaneity of the aggregating process

As disclosed above, the sand grains can aggregate together when being treated with P_4VP dispersion. Hence, it is highly possible that the aggregation process of treated sand grains is resulted from the spontaneous binding behavior of the adsorbed P_4VP molecules. Here, the P_4VP dimer has been adopted to explore the binding behavior between the P_4VP molecules. As a simple model, the geometries of the pyridine dimer consist of parallel-sandwich, antiparallel-sandwich, parallel-displaced, antiparallel-displaced, T-up and T-down, among which the antiparallel-displaced geometry tends to be the most stable (Hohenstein and Sherrill, 2009). It is expected that the P_4VP dimer should have the similar geometries to the pyridine dimer based on the structural similarity. However, due to steric hindrance, the P_4VP dimer can only be displayed approximate to antiparallel-displaced. The binding pyridine rings might be located in the middle (I) or one end (II) of the P_4VP molecules. The optimized configurations of two different binding modes (I, II) of P_4VP dimer, along with their binding energies are obtained as Fig. 12. The vertical separation between the stacking ring centers of the dimer I is 4.1 Å, which is slightly larger than that in the pyridine dimer (3.6 Å) (Mishra and Sathyamurthy, 2005). The increased ring spacing might result from the steric hindrance in P_4VP molecules. Notably, the binding energy of the dimer I is negative ($\Delta E_I = -23.76$ kJ/mol). The negative binding energy means the dimerization of P_4VP molecules is energetically favorable and spontaneous, which contributes to the self-aggregating behavior of P_4VP. A similar situation occurs in dimer II.

Although the dimerization of P_4VP molecules is energetically favorable and spontaneous, the P_4VP dimer can be broken due to the accelerated molecular thermal motion induced by high temperature (Liu et al., 2021). As the temperature falls, the P_4VP dimer will form again spontaneously to obtain the minimum energy. Hence, as presented in Fig. 7, the aggregation strength of the P_4VP-treated quartz microspheres can be weakened during the heating process and recovered during the cooling process, showing thermally reversible characteristics.

3.2.3. Essence of the intermolecular interaction between P_4VP dimer

Generally, the RDG method is adopted to distinguish the types and strength of interaction by providing information about

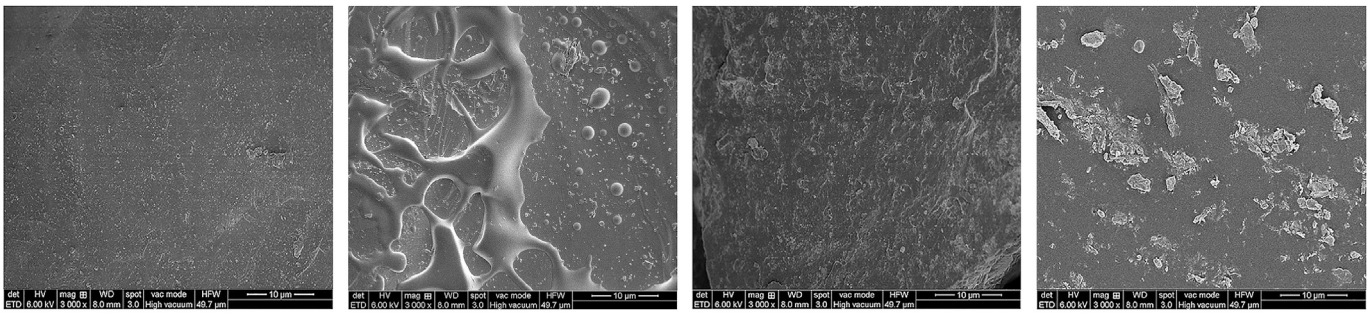

(a) Before treatment **(b)** After treatment, pH = 5 **(c)** After treatment, pH = 2 **(d)** After treatment, pH = 12

Fig. 9. Surface morphology of sand grains.

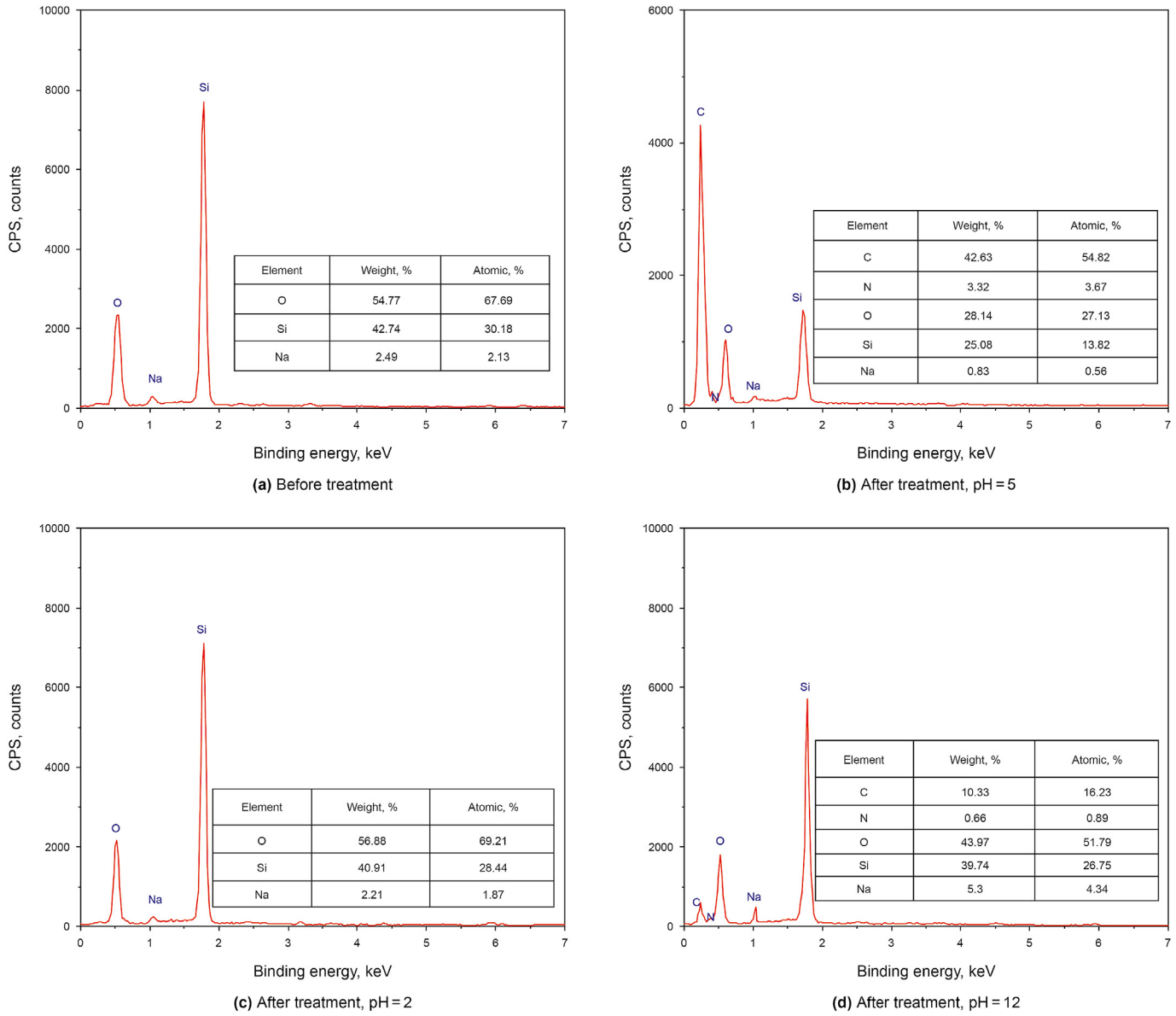

(a) Before treatment **(b)** After treatment, pH = 5

(c) After treatment, pH = 2 **(d)** After treatment, pH = 12

Fig. 10. Surface elemental composition of the sand grains.

intramolecular and intermolecular interactions (Venkataramanan et at., 2018). Here, the RDG method is employed to reveal the essence of the interaction between the binding pyridine rings in P_4VP dimer. Fig. 13 shows the plots of the reduced density (s) versus electron density (ρ) of P_4VP dimers (I, II). As displayed, a distinct spike occurs in the low-density, low-gradient region of the both

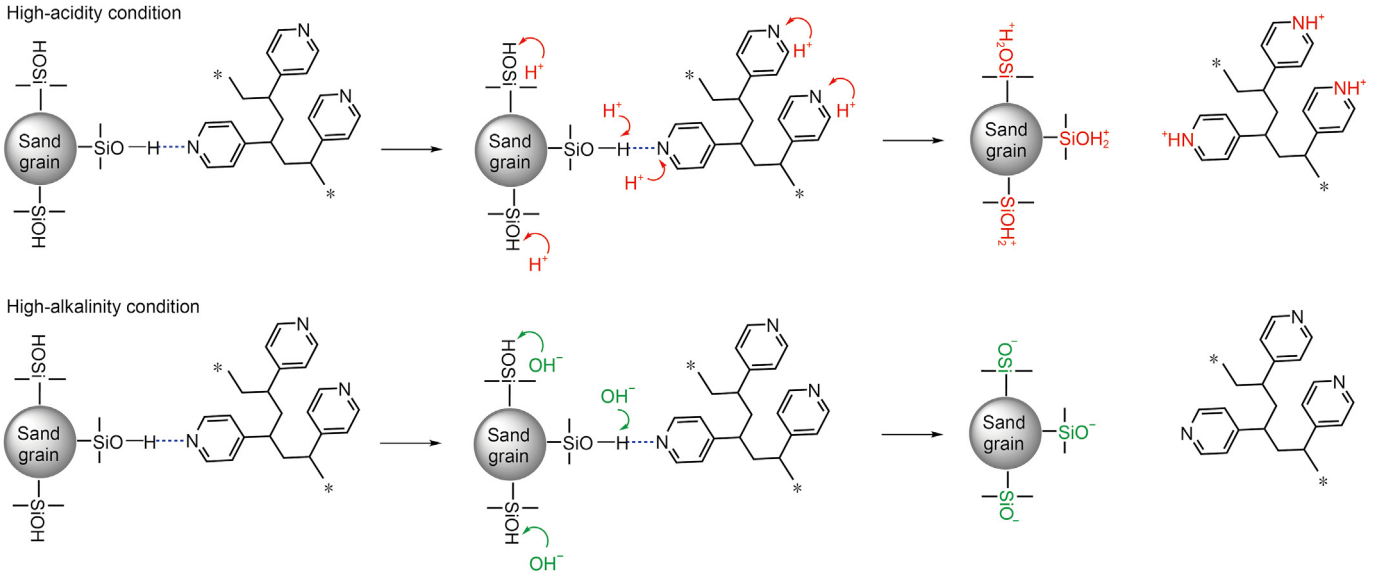

Fig. 11. Adsorption and desorption process of P_4VP.

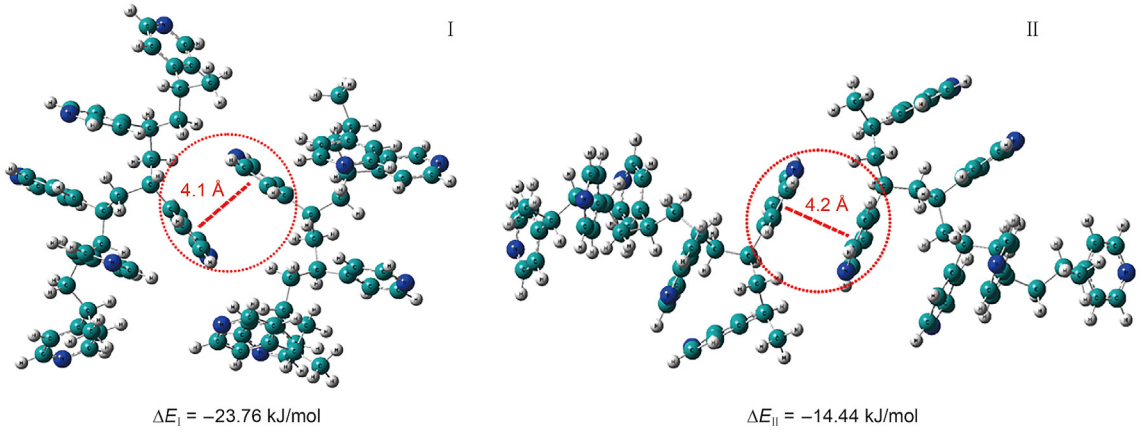

Fig. 12. Optimized configurations and binding energies of P_4VP dimers.

scatter diagrams, which signifies the existence of the noncovalent interactions (Johnson and Keinan, 2010). In RDG method, the weak interactions are categorized by the color of the gradient isosurfaces using color-coding with a blue-green-red scale (Li et al., 2022). As can be seen in Fig. 14, a green isosurface (encircled by the cube) occurs between the overlapping portions of the pyridine rings, where van der Waals (VDW) interaction is expected. Grimme has well demonstrated that dispersion interaction between spatially close-lying *p* electrons of unsaturated molecules in the stacked orientation is the essence of the π-π stacking effect (Grimme, 2008). According to this argument, the VDW interaction between the binding pyridine rings in P_4VP can be unambiguously identified as a typical π-π stacking effect.

The P_4VP molecules can combine with each other to form a stable dimer through π-π stacking interaction. Due to the broad interaction zone and the approximate antiparallel-displaced arrangement, the binding energies of P_4VP dimer can reach as high as −23.76 kJ/mol and −14.44 kJ/mol in both binding modes. It can be anticipated that there should be many more stacking dimers or even multimers in a certain concentration, which will contribute to the self-aggregating behavior of P_4VP.

3.3. Sand migration control performance

Adhesion force test and RDG analysis reveal that the P_4VP-treated sand grains will aggregate together through π-π stacking interaction to withstand the drag forces sufficiently. Hence, it is predictable that the formation sands production will be mitigated when treated with P_4VP dispersion. Sand pack displacement tests are conducted to evaluate the dynamic sand stabilization performance of the P_4VP dispersion. The P_4VP-treated sand packs are saturated with mineral oil and aqueous solution of different pH values separately and then displaced with 2 wt% KCl brine. Fig. 15 illuminates the MSFR of the treated sand packs at different temperatures. The unconsolidated sand pack is adopted as a blank group (MSFR: 5 mL/min, permeability retention rate: 100%). As presented, the MSFR of the treated sand packs can be substantially increased to 155–190 mL/min at 20 °C within the pH range of 4–8. Noteworthily, the MSFR barely changes when the sand pack is saturated by the mineral oil compared to that by the neutral or weakly acid aqueous solution, avoiding the risk of consolidation failure when the formation sands exposed to oil. Although the aggregation strength of sand grains decreases with the increasing

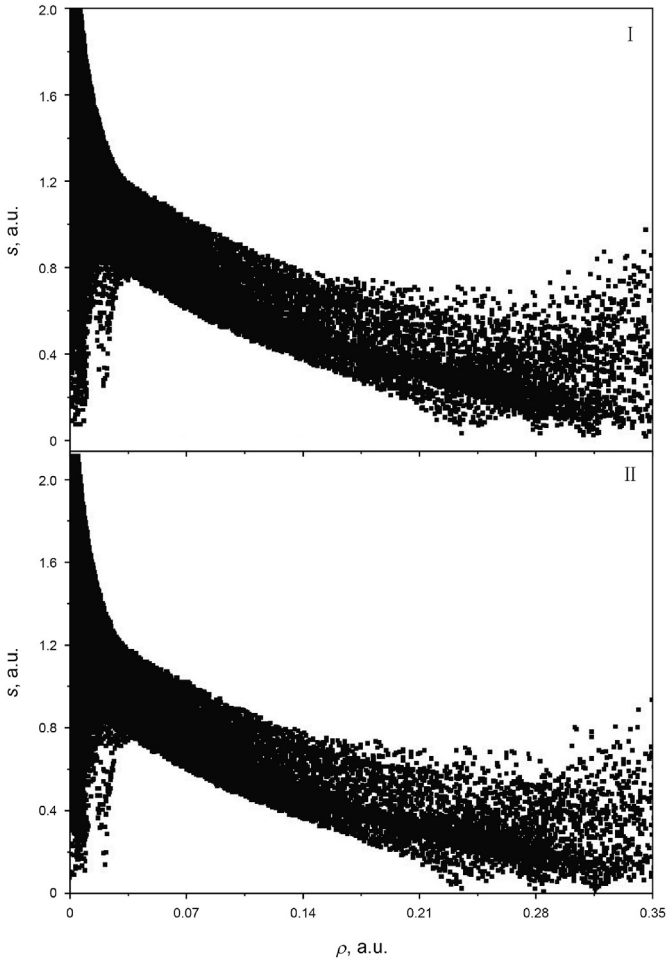

Fig. 13. Plots of the reduced gradient versus electron density of P_4VP dimers.

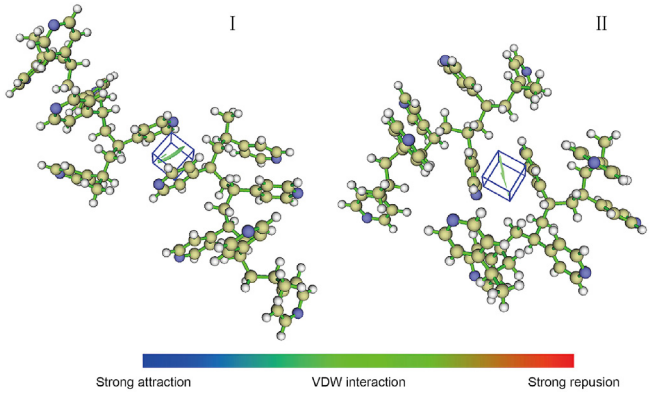

Fig. 14. Gradient isosurfaces for both types of P_4VP dimers.

temperature due to the structure failure of P_4VP dimers or multimers, the MSFR can still be maintained at 30–65 mL/min at 130 °C and mitigates the sand production effectively. As disclosed in Subsection 3.2.1, P_4VP can adsorb on the sand grains and significantly improves the MSFR by forming π-π stacking interactions in moderate pH conditions. Noteworthily, that the overall MSFR of sand packs at pH = 4–5 is higher than that of other pH values. The surface silanol groups on sand grains are mainly present as Si–OH at pH = 4–5, ensuring sufficient hydrogen-bonging interactions between the adsorbed P_4VP layer and the sand grains, which in turn

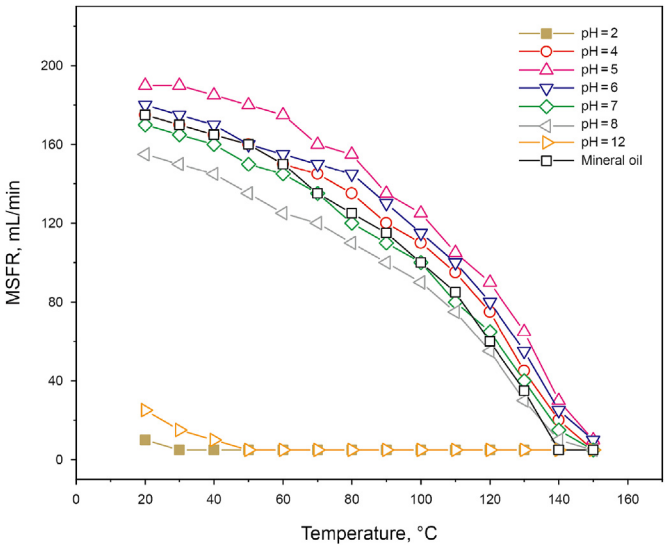

Fig. 15. The MSFR of the treated sand packs.

enhances the aggregation strength of sand grains and the MSFR (Malynych et al., 2002). Obviously, the P_4VP-treated sand packs are barely consolidated when pH = 2 in view that the MSFR drastically reduces to 10 mL/min at 20 °C. The protonated P_4VP will desorb from the sand grains and lead to the failure of the sand consolidation. A similar phenomenon occurs when pH = 12. The high-alkalinity condition leads to the complete rupture of the intermolecular hydrogen-bonding interactions between the sand grains and P_4VP molecules, resulting in the desorption of the P_4VP and the failure of the sand consolidation.

An effective injection fluid should be able to penetrate the formation matrix to a reasonable depth (Zhao and Bai, 2022; Dai et al., 2018). It is vital important to balance the consolidation strength with the permeability reduction in treated intervals. Penetration of the P_4VP dispersion in the formation depends on its viscosity and on the flow of the P_4VP dispersion into the formation matrix (Lahalih and Ghloum, 2010). The aqueous P_4VP dispersion possesses low viscosity (close to water) and small particle size (dozens of nanometers), hence, the regained permeability of the P_4VP-treated sand packs should be reliable. Fig. 16 illuminates the permeability retention rate of the P_4VP-treated sand packs in different pH conditions at 20 °C. Owing to the relatively weak physical consolidation, the permeability retention rate of the sand packs is up to 70.2%–86.7% at 20 °C within the pH range of 4–8. Although the permeability retention rate is close to 100% at pH = 2, the treated sand pack is barely consolidated due to the desorption of the P_4VP. The relatively low permeability retention rate at pH = 12 might result from the blocking by the deposit sediments generated from the desorbed P_4VP. In summary, the P_4VP dispersion shows wide pH and temperature ranges for application. The production of sands can be mitigated at 20–130 °C within the pH range of 4–8.

Although it is hard to define a benchmark for the adhesion force or MSFR for effective consolidation in view of different well/reservoir conditions, a fitted equation is provided and might provide a guidance for the field application. The experimental data is summarized from the adhesion force tests and the sand pack displacement tests (pH = 7) to further clear the influence of the adhesion force on the MSFR. The temperature and the mass fraction of P_4VP dispersion are adopted as variables. It is understandable that the adhesion force and the corresponding MSFR both increase with the mass fraction of P_4VP dispersion (Fig. 17). Then fitting

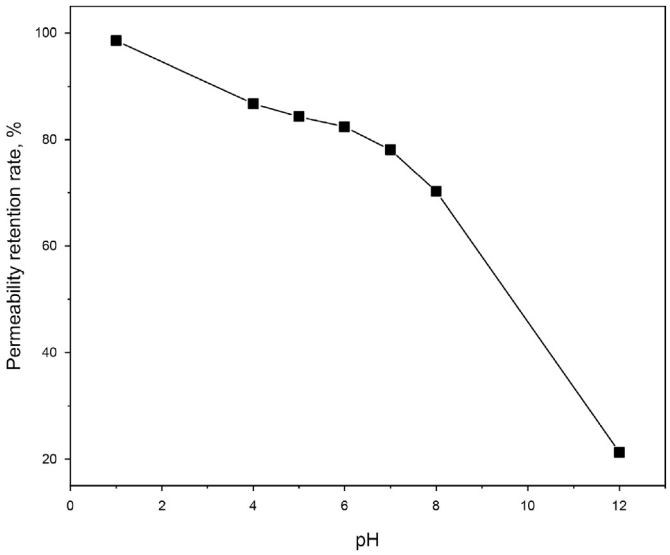

Fig. 16. The permeability retention rate of the treated sand packs.

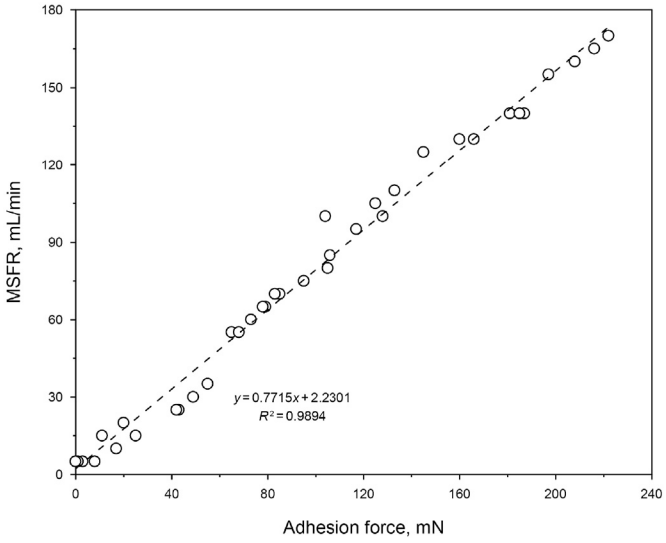

Fig. 18. Relationship of the MSFR with the adhesion force.

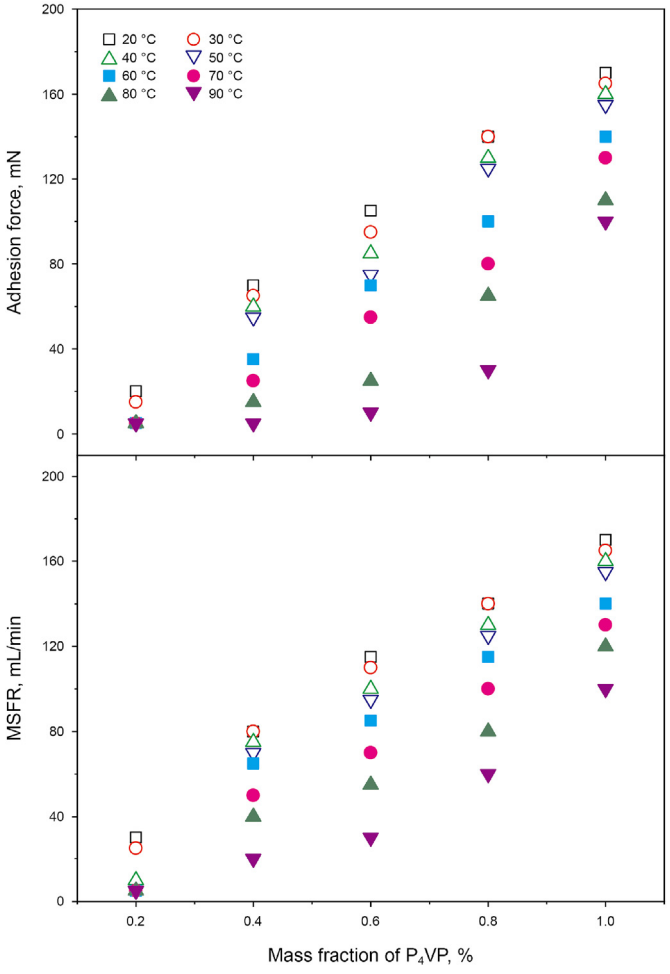

Fig. 17. The adhesion force and the MSFR variation with the mass fraction of P_4VP dispersion and temperature.

process is conducted in Fig. 18. As presented, the MSFR of the treated sand pack is linearly varying with the adhesion force. The fitted equation is authenticated by the experimental data in different pH conditions at 20 °C (Figs. 7 and 15) and proved to be reasonable. With the aid of the fitted equation, it is feasible to adjust the mass fraction or even the injection volume of the P_4VP dispersion to obtain a certain MSFR to meet the requirement of the target reservoir.

4. Conclusions

We proposed the poly(4-vinyl pyridine) (P_4VP) for sand migration control. The self-aggregating behavior of the P_4VP as well as the aggregation strength between the treated sand grains were characterized by adhesion force test. Influential factors on the aggregation strength of the treated sand grains were evaluated at different pH and temperature conditions. The adsorption as well as the desorption behavior of P_4VP on sand grains was characterized by scanning electron microscopy and adhesion force test. The intermolecular interaction between P_4VP molecules was analyzed by reduced density gradient analysis. The static stability of the P_4VP dispersion is evaluated by dynamic light scattering. The sand migration control performance of the P_4VP dispersion was revealed by dynamic sand stabilization test. The results indicated that:

(1) The P_4VP could aggregate sand grains spontaneously to withstand the drag forces sufficiently.
(2) The pH condition altered the forms of surface silanol groups on sand grains which in turn affected the adsorption behavior of the P_4VP.
(3) The spontaneous dimerization of P_4VP was resulted from the π-π stacking interaction, which contributed to the self-aggregating behavior and the thermally reversible characteristics of the P_4VP.
(4) The P_4VP dispersion showed wide pH and temperature ranges of application. The production of sands can be mitigated at 20–130 °C under the pH condition of 4–8.
(5) The fitted equation related to the MSFR and the adhesion force can be used as a reference for the formula design to adapt to the specific well/reservoir condition.

Acknowledgments

The authors gratefully appreciate the support from the National Key R&D Program of China (grant number 2018YFA0702400), the

Major Scientific and Technological Projects of CNPC (grant number ZD2019-183-007) and the China Postdoctoral Science Foundation (grant number 2021M702041).

References

Abanum, A.M., Appah, D., 2013. Laboratory studies of chemicals for sand consolidation (Scon) in the Niger Delta fields. In: SPE Nigeria Annual International Conference and Exhibition. https://doi.org/10.2118/167516-MS.

Alakbari, F.S., Mohyaldinn, M.E., Muhsan, A.S., Hasan, N., Ganat, T., 2020. Chemical sand consolidation: from polymers to nanoparticles. Polymers 12, 1069. https://doi.org/10.3390/polym12051069.

Albadi, J., Keshavarz, M., Abedini, M., Vafaie-nezhad, M., 2012. Copper iodide nanoparticles on poly(4-vinyl pyridine) as new and green catalyst for multicomponent click synthesis of 1,4-disubstituted-1,2,3-triazoles in water. Chin. Chem. Lett. 23, 797–800. https://doi.org/10.1016/j.cclet.2012.05.009.

Arslan, M., Saraydin, D., 2017. Radiation-induced acrylamide/4-vinyl pyridine biocidal hydrogels: synthesis, characterization, and antimicrobial activities. Polym. Plast. Technol. Eng. 56, 1295–1306. https://doi.org/10.1080/03602559.2016.1275683.

Chaloupka, V., Riyanto, L., Tran, Q., Rayne, A.S., Haekal, M., Kristanto, T., 2010. Remedial sand consolidation: case study from Mahakam Delta, Indonesia. In: SPE International Symposium and Exhibition on Formation Damage Control. https://doi.org/10.2118/127489-MS.

Chetia, J.R., Moulick, M., Dutta, A., 2004. Preparation, characterization and conductivity measurement of poly(4-vinyl pyridinium) salts in solid state. Indian J. Chem. Technol. 11, 80–84. https://doi.org/10.1039/9781847551214-00589.

Dai, C.L., Zou, C.W., Liu, Y.F., You, Q., Tong, Y., Wu, C., Shan, C.H., 2018. Matching principle and in-depth profile control mechanism between elastic dispersed particle gel and pore throat. Acta Pet. Sin. 39, 427–434. https://doi.org/10.7623/syxb201804006 (in Chinese).

Dupuis, G., Bouillot, J., Zaitoun, A., Caremi, G., Burrafato, G., 2016. Combined water/sand control polymer treatments in offshore gas wells. In: SPE EOR Conference at Oil and Gas West Asia. https://doi.org/10.2118/179825-MS.

Frisch, M.J., Trucks, G.W., Schlegel, H.B., Scuseria, G.E., Robb, M.A., Cheeseman, J.R., et al., 2009. Gaussian 09W, Version 7.0.

Fujii, S., Kameyama, S., Armes, S.P., Dupin, D., Suzaki, M., Nakamura, Y., 2010. pH-responsive liquid marbles stabilized with poly(2-vinylpyridine) particles. Soft Matter 6, 635–640. https://doi.org/10.1039/b914997j, 635.

Fuller, M.J., Gomez, R.A., Gill, J., 2011. Development of new sand consolidation fluid and field application in shallow gas reservoirs. In: SPE Asia Pacific Oil and Gas Conference and Exhibition. https://doi.org/10.2118/145409-MS.

Grimme, S., 2008. Do special noncovalent π-π stacking interactions really exist? Angew. Chem. Int. Ed. 47, 3430–3434. https://doi.org/10.1002/anie.200705157.

Hafez, I.T., Paraskeva, C.A., Klepetsanis, P.G., Koutsoukos, P.G., 2011. Sand consolidation with calcium phosphate-polyelectrolyte composites. J. Colloid Interface Sci. 363, 145–156. https://doi.org/10.1016/j.jcis.2011.07.048.

Hohenstein, E.G., Sherrill, C.D., 2009. Effects of heteroatoms on aromatic π-π interactions: benzene-pyridine and pyridine dimer. J. Phys. Chem. 113, 878–886. https://doi.org/10.1021/jp809062x.

Huang, Y., Xie, A., Seidi, F., Zhu, W.Y., Li, H., Yin, S., Xu, X., Xiao, H.N., 2021. Core-shell heterostructured nanofibers consisting of Fe_7S_8 nanoparticles embedded into S-doped carbon nanoshells for superior electromagnetic wave absorption. Chem. Eng. J. 423, 130307. https://doi.org/10.1016/j.cej.2021.130307.

Humphrey, W., Dalke, A., Schulten, K., 1996. VMD: visual molecular dynamics. J. Mol. Graph. 14, 33–38. https://doi.org/10.1016/0263-7855(96)00018-5.

İşoğlu1, İ.A., Demirkan, C., Şeker, M.G., Tuzlakoğlu, K., İşoğlu1, S.D., 2018. Antibacterial bilayered skin patches made of HPAM and quaternary poly(4-vinyl pyridine). Fibers Polym. 19, 2229–2236. https://doi.org/10.1007/s12221-018-8480-9.

Johnson, E.R., Keinan, S., Mori-Sánchez, P., Contreras-Garcıá, J., Cohen, A.J., Yang, W.T., 2010. Revealing noncovalent interactions. J. Am. Chem. Soc. 132, 6498–6506. https://doi.org/10.1021/ja100936w.

Kalgaonkar, R., Chang, F., Ballan, A.A., Abadi, A., Tan, X.Y., 2017. New advancements in mitigating sand production in unconsolidated formations. In: SPE Kingdom of Saudi Arabia Annual Technical Symposium and Exhibition. https://doi.org/10.2118/188043-MS.

Kawabata, N., Ohira, K., 1979. Removal and recovery of organic pollutants from aquatic environment. 1. Vinylpyridine-divinylbenzene copolymer as a polymeric adsorbent for removal and recovery of phenol from aqueous solution. Environ. Sci. Technol. 13, 1396–1402. https://doi.org/10.1021/es60159a015.

Kuma, P., Affeld, C.J., 2018. Experience with chemical sand consolidation: case studies from west Africa. In: SPE Offshore Technology Conference. https://doi.org/10.4043/28267-MS.

Lahalih, S.M., Ghloum, E.F., 2010. Polymer compositions for sand consolidation in oil wells. In: SPE Production and Operations Conference and Exhibition. https://doi.org/10.2118/136024-MS.

Li, F.C., Zheng, Z.J., Xia, S.W., Yu, L.M., 2020. Synthesis, co-crystal structure, and DFT calculations of a multicomponent co-crystal constructed from 1H-benzotriazole and tetrafluoroterephthalic acid. J. Mol. Struct. 1219, 128480. https://doi.org/10.1016/j.molstruc.2020.128480.

Li, H., Guo, J.J., Zhang, Y.H., Zhao, L., Gao, J.S., Xu, C.M., 2022. Research on separation of aromatics from FCC diesel using organic solvent: a combination of experiments and quantum chemical calculations. Fuel 308, 121982. https://doi.org/10.1016/j.fuel.2021.121982.

Li, X.Q., Zhang, G.C., Ge, J.J., Qi, N., Jiang, P., Liao, K.L., Qiao, W.L., 2017. Organosilane film for sand migration control based on in-situ hydrolysis and polycondensation effects. J. Petrol. Sci. Eng. 158, 660–671. https://doi.org/10.1016/j.petrol.2017.08.013.

Liu, D.X., Zhong, X., Shi, X.F., Qi, Y.J., Zhu, T.Y., Shao, M.L., Zhang, F., 2016. Pentaerythritol phosphate melamine salt, a new aggregating reagent for oilfield chemical sand control preparation, properties, and mechanism. Energy Fuels 30, 2503–2513. https://doi.org/10.1021/acs.energyfuels.5b02648.

Liu, Z.Y., Lu, T., Chen, Q.X., 2021. Intermolecular interaction characteristics of the all-carboatomic ring, cyclo[18]carbon: focusing on molecular adsorption and stacking. Carbon 171, 514–523. https://doi.org/10.1016/j.carbon.2020.09.048.

Lu, T., Chen, F.W., 2012. Multiwfn: a multifunctional wavefunction analyzer. J. Comput. Chem. 33, 580–592. https://doi.org/10.1002/jcc.22885.

Ma, C.Y., Deng, J., Dong, X.L., Sun, D.Z., Feng, Z., Luo, C., Xiao, Q.Z., Chen, J.Y., 2020. A new laboratory protocol to study the plugging and sand control performance of sand control screen. J. Petrol. Sci. Eng. 184, 106548. https://doi.org/10.1016/j.petrol.2019.106548.

Mahardhini, A., Abidiy, I., Poitrenaud, H., Wiendyahwati, S., Mayasari, F., Wood, T., Magee, C., 2015. Chemical sand consolidation as a failed gravel pack sand-control remediation on Handil field, Indonesia. In: SPE European Formation Damage Conference and Exhibition. https://doi.org/10.2118/174240-MS.

Malynych, S., Luzinov, I., Chumanov, G., 2002. Poly(vinyl pyridine) as a universal surface modifier for immobilization of nanoparticles. J. Phys. Chem. B 106, 1280–1285. https://doi.org/10.1021/jp013236d.

Marandia, S.Z., Salehib, M.B., Moghadam, A.M., 2018. Sand control: experimental performance of polyacrylamide hydrogels. J. Petrol. Sci. Eng. 170, 430–439. https://doi.org/10.1016/j.petrol.2018.06.074.

Marfo, S.A., Appah, D., Joel, O.F., 2015. Sand consolidation operations, challenges and remedy. In: SPE Nigeria Annual International Conference and Exhibition. https://doi.org/10.2118/178306-MS.

Mishra, B.K., Sathyamurthy, N., 2005. π-π interaction in pyridine. J. Phys. Chem. 109, 6–8. https://doi.org/10.1021/jp045218c.

Mishra, S., Ojha, K., 2016. Nanoparticle induced chemical system for consolidating loosely bound sand formations in oilfields. J. Petrol. Sci. Eng. 147, 15–23. https://doi.org/10.1016/j.petrol.2016.05.005.

Ogolo, N.A., 2013. The trapping capacity of nanofluids on migrating fines in sand. In: SPE Annual Technical Conference and Exhibition. https://doi.org/10.2118/167632-STU.

Ott, W.K., Woods, J.D., 2003. Modern Sandface Completion Practices Handbook, first ed. Gulf Publishing Company, Houston.

Ranjith, P.G., Perera, M.S.A., Perera, W.K.G., Wub, B., Choi, S.K., 2013. Effective parameters for sand production in unconsolidated formations: an experimental study. J. Petrol. Sci. Eng. 105, 34–42. https://doi.org/10.1016/j.petrol.2013.03.023.

Son, S.Y., Kim, J., Song, E., Choi, K., Lee, J., Cho, K., Kim, T., Park, T., 2018. Exploiting π-π stacking for stretchable semiconducting polymers. Macromolecules 51, 2572–2579. https://doi.org/10.1021/acs.macromol.8b00093.

Song, J.H., Couzis, A., Lee, J.W., 2010. Direct measurements of contact force between clathrate hydrates and water. Langmuir 26, 9187–9190. https://doi.org/10.1021/la101309j.

Stachera, D.M., Childs, R.F., 2001. Tuning the acid recovery performance of poly(4-vinylpyridine) -filled membranes by the introduction of hydrophobic groups. J. Membr. Sci. 187, 213–225. https://doi.org/10.1016/S0376-7388(01)00349-0.

Styward, B., Wijaya, R., Manalu, D., 2018. Sand conglomeration trial as an alternative to sand control case study from Mahakam Delta, Indonesia. In: SPE Asia Pacific Oil and Gas Conference and Exhibition. https://doi.org/10.2118/191987-MS.

Tabbakhzadeh, M.N., Esmaeilzadeh, F., Zabihi, R., Mowla, D., 2020. Experimental study of chemical sand consolidation using epoxy and furan resins for oil wells: experimental design models. Int. J. Rock Mech. Min. Sci. 135, 104486. https://doi.org/10.1016/j.ijrmms.2020.104486.

Talaghat, M.R., Esmaeilzadeh, F., Mowla, D., 2009. Sand production control by chemical consolidation. J. Petrol. Sci. Eng. 67, 34–40. https://doi.org/10.1016/j.petrol.2009.02.005.

Tantavichet, N., Pritzker, M.D., Burns, C.M., 2001. Proton uptake by poly(2-vinylpyridine) coatings. J. Appl. Polym. Sci. 81 (6), 1493–1497. https://doi.org/10.1002/app.1577.

Venkataramanan, N.S., Suvitha, A., Kawazoe, Y., 2018. Unravelling the nature of binding of cubane and substituted cubanes within cucurbiturils: a DFT and NCI study. J. Mol. Liq. 260, 18–29. https://doi.org/10.1016/j.molliq.2018.03.071.

Wang, S.Q., Zhao, J., 2007. First-order conformation transition of single poly(2-vinylpyridine) molecules in aqueous solutions. J. Chem. Phys. 126, 091104. https://doi.org/10.1063/1.2711804.

Zaitoun, A., Pichery, T.R., 2009. New polymer technology for sand control treatments of gas storage wells. In: SPE International Symposium on Oilfield Chemistry. https://doi.org/10.2118/121291-MS.

Zhao, F.L., 2001. EOR Principles, first ed. China university of petroleum Press, Dongying (in Chinese).

Zhao, Y., Bai, B.J., 2022. Selective penetration behavior of microgels in super-permeable channels and reservoir matrices. J. Petrol. Sci. Eng. 210, 109897. https://doi.org/10.1016/j.petrol.2021.109897.